Edith Cowan University

Research Online

Research outputs 2022 to 2026

9-1-2023

Enhancing the CO2 trapping capacity of Saudi Arabian basalt via nanofluid treatment: Implications for CO2 geo-storage

Muhammad Ali

Nurudeen Yekeen
Edith Cowan University

Mirhasan Hosseini
Edith Cowan University

Ghazanfer R. Abbasi
Edith Cowan University

Amer Alanazi

See next page for additional authors

Follow this and additional works at: https://ro.ecu.edu.au/ecuworks2022-2026

 Part of the Geotechnical Engineering Commons

10.1016/j.chemosphere.2023.139135
Ali, M., Yekeen, N., Hosseini, M., Abbasi, G. R., Alanazi, A., Keshavarz, A., . . . Hoteit, H. (2023). Enhancing the CO2 trapping capacity of Saudi Arabian basalt via nanofluid treatment: Implications for CO2 geo-storage. Chemosphere, 335, article 139135. https://doi.org/10.1016/j.chemosphere.2023.139135
This Journal Article is posted at Research Online.
https://ro.ecu.edu.au/ecuworks2022-2026/2551

Authors

Muhammad Ali, Nurudeen Yekeen, Mirhasan Hosseini, Ghazanfer R. Abbasi, Amer Alanazi, Alireza Keshavarz, Thomas Finkbeiner, and Hussein Hoteit

This journal article is available at Research Online: https://ro.ecu.edu.au/ecuworks2022-2026/2551

Chemosphere 335 (2023) 139135

Contents lists available at ScienceDirect

Chemosphere

journal homepage: www.elsevier.com/locate/chemosphere

Enhancing the CO_2 trapping capacity of Saudi Arabian basalt via nanofluid treatment: Implications for CO_2 geo-storage

Muhammad Ali [a,*], Nurudeen Yekeen [b], Mirhasan Hosseini [b], Ghazanfer Raza Abbasi [b], Amer Alanazi [a], Alireza Keshavarz [b], Thomas Finkbeiner [a], Hussein Hoteit [a,**]

[a] Physical Science and Engineering Division, King Abdullah University of Science and Technology (KAUST), Thuwal, 23955, Saudi Arabia
[b] School of Engineering, Edith Cowan University, Joondalup, 6027, Western Australia, Australia

HIGHLIGHTS

- At all tested pressure and temperature conditions the Pure Saudi Arabian (SA) basalt is water-wet.
- SA basalt turned into hydrophobic in the presence of organic acids.
- 0.1 wt% SiO_2 nanofluid concentration have shown optimum results for shifting the CO_2-wettability to water-wet conditions.
- Nanofluids have increased the CO_2 column heights which were lower in organic-aged SA basalt.

GRAPHICAL ABSTRACT

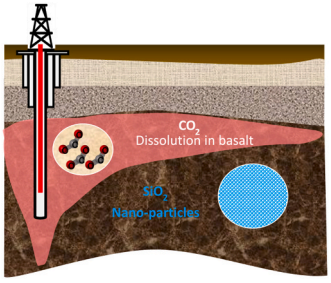

ARTICLE INFO

Handling Editor: Muhammad Mubashir

Keywords:
CO_2 geo-storage
CO_2 wettability
SiO_2 nanofluids
Saudi arabian basalt
Organic acid
CO_2 column heights

ABSTRACT

Mineralization reactions in basaltic formations have gained recent interest as an effective method for CO_2 geo-storage in order to mitigate anthropogenic greenhouse gas emissions. The CO_2/rock interactions, including interfacial tension and wettability, are crucial factors in determining the CO_2 trapping capacity and the feasibility of CO_2 geological storage in these formations. The Red Sea geological coast in Saudi Arabia has many basaltic formations, and their wetting characteristics are rarely reported in the literature. Moreover, organic acid contamination is inherent in geo-storage formations and significantly impacts their CO_2 geo-storage capacities. Hence, to reverse the organic effect, the influence of various SiO_2 nanofluid concentrations (0.05–0.75 wt%) on the CO_2-wettability of organic-acid aged Saudi Arabian (SA) basalt is evaluated herein at 323 K and various pressures (0.1–20 MPa) via contact angle measurements. The SA basalt substrates are characterized via various techniques, including atomic force microscopy, energy dispersive spectroscopy, scanning electron microscopy, and others. In addition, the CO_2 column heights that correspond to the capillary entry pressure before and after nanofluid treatment are calculated. The results show that the organic acid-aged SA basalt substrates become intermediate-wet to CO_2-wet under reservoir pressure and temperature conditions. When treated with SiO_2 nanofluids, however, the SA basalt substrates become weakly water-wet, and the optimum performance is observed at an SiO_2 nanofluid concentration of 0.1 wt%. At 323 K and 20 MPa, the CO_2 column height corresponding to the capillary entry pressure increases from −957 m for the organic-aged SA basalt to 6253 m for the 0.1 wt% nano-treated SA basalt. The results suggest that the CO_2 containment security of organic-acid-

* Corresponding author.
** Corresponding author.
E-mail addresses: Muhammad.ali.2@kaust.edu.sa (M. Ali), Hussein.hoteit@kaust.edu.sa (H. Hoteit).

https://doi.org/10.1016/j.chemosphere.2023.139135
Received 24 April 2023; Received in revised form 11 May 2023; Accepted 3 June 2023
Available online 5 June 2023
0045-6535/© 2023 The Authors. Published by Elsevier Ltd. This is an open access article under the CC BY license (http://creativecommons.org/licenses/by/4.0/).

contaminated SA basalt can be enhanced by SiO_2 nanofluid treatment. Thus, the results of this study may play a significant role in assessing the trapping of CO_2 in SA basaltic formations.

1. Introduction

Intense efforts are currently focused on attaining net zero carbon emissions globally (M. Blunt et al., 1993; Ali et al., 2022a; Aslannezhad et al., 2023). Many nations of the world have indicated their interest in ensuring that the rate of CO_2 gas emission should be restricted or eliminated by 2050 (Wang et al., 2020; Bamisile et al., 2022; Khalifa et al., 2022). Carbon capture, utilization, and sequestration in saline caverns and aquifers, as well as depleted oil and gas reservoirs, has been proposed as a practical technique for achieving net zero carbon emissions (Ali et al., 2017, 2020a; Ali, 2018, 2021; Delshad et al., 2022; Raad et al., 2022). In this respect, tight carbonates and sandstone, organic-rich shales, gas hydrates, and basaltic rocks have recently been recognized as prominent CO_2 storage basins (Gislason et al., 2010; Mahesar et al., 2020; Torres, 2020; Al-Yaseri et al., 2021b; Abbasi et al., 2022; Hosseini et al., 2022a; Oelkers et al., 2022).

Basalts are fine-grained, dark-colored, mafic rocks that contain various minerals such as olivine, pyroxene, augite, anorthite, albite, and plagioclase. Basaltic rocks are abundantly present worldwide, especially near sea-bed areas (Torres, 2020; Oelkers et al., 2022). One of the most critical areas of alkali olivine basalt in the world, covering almost 90, 000 km^2, is the Cenozoic volcanic rock area of Saudi Arabia (SA) (Coleman et al., 1983; Arkadakskiy et al., 2020), a leading oil-producing nation and a significant contributor to anthropogenic CO_2 emissions through fossil fuel consumption (Agboola et al., 2021; Hamieh et al., 2022). Part of the anticipated CO_2 release from fossil fuel burning could be safely stored in these basaltic formations to achieve the net zero carbon emission target (Ali et al., 2023).

The primary CO_2 trapping mechanism in basaltic rocks is carbon mineralization (Kang et al., 2018; Kelemen et al., 2019; Cao et al., 2020). Compared to sandstone, basalt reacts more strongly with brine that is saturated with acidified CO_2 (Iglauer et al., 2020; Al-Yaseri et al., 2021b), thus making the mineral trapping of CO_2 in basaltic formations highly promising (Snæbjörnsdóttir et al., 2014; Arkadakskiy et al., 2020; Raza et al., 2022). For example, almost 95% of the injected CO_2 became mineralized in less than 24 months of injection into Icelandic basalts during the Carbfix CO_2 sequestration project, with only slightly lower efficiency than observed in the Columbia River Basalt (Matter et al., 2016; Iglauer et al., 2020; Al-Yaseri et al., 2021b).

An important CO_2 storage mechanism depends on the rock/CO_2/brine interactions, which are governed by the rock-wetting behaviors and rock-fluid interfacial tensions (Al-Khdheeawi et al., 2020, 2021; Al-Mukainah et al., 2022; Al-Yaseri et al., 2022; Ali et al., 2017; Al-Yaseri et al., 2021; Al-Anssari et al., 2020). The presence of organic acids in geo-storage formations, including basalts, significantly affects their wettabilities and, hence, their CO_2 trapping capacities (Hosseini et al., 2022a; Ali et al., 2023). Hence, an examination of the CO_2 wetting characteristics of SA basalt can provide an insight into the interfacial area available for mass exchange that could increase the extent of mineralization (Al-Yaseri et al., 2021a). Previous studies (including experiments and molecular dynamic simulations) have evaluated the storage capacities of geological formations by assessing the rock/-CO_2/brine interactions (Bikkina, 2011; Farokhpoor et al., 2013a; Wang et al., 2016; Arif et al., 2017; Daryasafar et al., 2019; Silvestri et al., 2019; Le et al., 2020; Yekeen et al., 2020), along with the sealing integrities of the caprocks at various temperatures, pressures, salinities, and contents of organic acids in the geo-storage formations (Ali et al., 2019a, 2019b, 2022b; Abdulelah et al., 2021; Yekeen et al., 2021; Hosseini et al., 2022b). However, compared to other conventional storage rocks such as sandstone and carbonates, the wetting behavior of basalt during CO_2 storage has been least investigated. Only a handful of studies have evaluated the wetting characteristics of basaltic formations (Iglauer et al., 2020; Al-Yaseri et al., 2021b; Raza et al., 2022; Ali et al., 2023). For example (Ali et al., 2023), demonstrated that pure SA basalt has hydrophilic characteristics, whereas SA basalt substrates aged in small concentrations of organic acid become more hydrophobic. It has been also proven that geo-storage formations have even higher concentrations of organics, which may adversely affect the CO_2 trapping capacities and mineralization reactions (Lundegard and Kharaka, 1994; Jones et al., 2008; Akob et al., 2015).

In the present study, various concentrations of SiO_2 nanofluid (0.05–0.75 wt% dispersed in 0.3 M NaCl solution) are applied to organic-aged SA basalt samples. The corresponding advancing and receding contact angles are then measured and compared with those of the untreated, organic-aged SA basalt sample at 323 K and various pressures (0.1–20 MPa) in order to comprehend the wettability reversing effect. After identifying the optimum nanofluid concentration, the CO_2 column heights are calculated in order to determine the enhancement in the CO_2 trapping capacity of the SA basalt due to the nanofluid aging. The results of this study are expected to aid in enhancing the CO_2 geo-storage capacities of SA basaltic formations.

2. Materials and methods

2.1. Materials

The basalt samples were collected from the Harrat Rahat area, near the Red Sea coast of western SA (Moufti and Németh, 2016). The stearic acid (99.5% purity, pH = 6) and n-decane were acquired from Sigma Aldrich. The hydrophilic, nearly spherical, and porous nanosilica (SiO_2; purity $\geq$ 99.50%) was also supplied by Sigma Aldrich (Awan et al., 2021). Sodium chloride (NaCl; purity = 99.999%) was obtained from Rowe Scientific to prepare the 0.3 M brine solution for contact angle measurements, and de-ionized (DI) water (Ultrapure; electrical conductivity = 0.02 mS/cm) was obtained from David Gray. Ultra-pure nitrogen (N_2; purity 99.999%) and carbon dioxide (CO_2; purity 99.999%) were acquired from BOC Australia. Dilute hydrochloric acid (37.5 wt%) was obtained from Sigma Aldrich and other solvents (methanol, toluene, and acetone; purity = 99.999%) were acquired from Rowe Scientific.

2.2. The organic-acid and nanofluid aging processes

Initially, SA basalt substrates were cleaned with DI water and ultra-pure nitrogen, followed by immersing them in the brine solution (2 wt %) pre-equilibrated at pH 4 with aqueous droplets of 37.5 wt% dilute HCl for 30 min in order to ensure the ionization of the basalt surface, thereby enhancing the adsorption of organic acid molecules (Ali, 2018, 2021; Ali et al., 2022c, 2022d). Ultra-pure nitrogen was then used to remove the thin films of brine from the surface of the basalt prior to immersion in 1:5 n-decane/stearic acid solution (10^{-2} mol/L) on the gram scale. The solution was left to stand for 7 days at 323 K to mimic the basalt surface exposure to formation brines under geo-storage conditions (Ali et al., 2021c, 2021d, 2022d; Iglauer et al., 2021). The esterification of the –OH groups on the surface of the basalt by the organic acid promoted the hydrophobicity of the basalt surface via covalent bonding, as shown in Fig. 1.

The nanofluid dispersions with various concentrations of SiO_2 (0.05–0.75 wt%) were prepared by adding the desired mass in grams to the 0.3 M NaCl solutions and subjecting to ultrasonic homogenization (Sonics and Materials Incorporation, USA) at a frequency of 20 kHz, an energy of 9500 J, and an amplitude of 40%, for 15 min. To prevent

overheating, 2 min rest periods were observed at 5-min intervals during the sonication process. The organic-aged SA basalt samples were then vertically submerged in the various nanofluids at 323 K and atmospheric pressure for 7 days. This aging procedure was similar to that reported in previous studies (Nwidee et al., 2016; Al-Anssari et al., 2018; Ali et al., 2020b, 2021a; Al-Yaseri et al., 2021a).

2.3. Contact angle measurements

Contact angle measurements directly provide information on the wettability of the rock–CO_2–brine system (Lander et al., 1993). In the present study, the contact angle measurements were performed on SA basalt thin sections that were prepared by cutting and polishing from the SA basalt chunks. The SA basalt samples were pre-equilibrated with CO_2 and brine (0.3 M NaCl) solution under the desired geo-storage conditions in a mixing reactor (Parr Instruments) at 1200 rpm to eliminate any mass-transfer effects due to the interactions of the basalt surface with the brine and CO_2 (El-Maghraby et al., 2012). The advancing and receding contact angles (θ_a and θ_r) were then measured at a constant temperature of 323 K and various pressures (0.1–20 MPa) via the tilted plate goniometric method (Lander et al., 1993; Iglauer, 2017). For this process, the substrate was placed in a viewing cell, then the surrounding fluid (ultra-pure CO_2) was injected via an ISCO pump (from ISCO, USA), and an equilibrated brine droplet (5.5 μL) was dispensed in a controlled manner via another ISCO pump. The contact angle measurements (θ_a and θ_r) were then recorded before droplet movement at the leading and trailing edges respectively. The procedure was recorded using a high-performance video camera, followed by processing with ImageJ software to extract the images for further quantification. All measurements were within the standard deviation range of ±3°. Similar methodologies for contact angle measurement were adopted in our previous research articles (Alhamad et al., 2022, 2023; Alanazi et al., 2023; Hosseini et al., 2023).

2.4. Characterization

The surface roughnesses of the basalt samples were determined via atomic force microscopy (AFM; Nano-surf, Flex-Axiom) with a C3000 controller. The pore throat radii and Brunauer–Emmett–Teller (BET) surface area were measured using a surface area and porosity analyzer (Micrometrics TriStar IIPlus-3030). The total organic carbon (TOC) contents of the pure and organic-aged basalt samples were obtained via pyrolysis using a Rock-Eval 6 apparatus (Vinci Technologies, France). The mineralogies of the pure SA basalt sample was examined via X-ray diffraction (XRD; Bruker D8 Discover Plus). The morphologies were examined via field emission scanning electron microscopy (FESEM; Oxford Instruments) equipped with energy dispersive spectroscopy (EDS) spectroscopy.

3. Results and discussion

3.1. Characterization of saudi Arabian (SA) basalt

The AFM images and surface roughness profiles of the pure (un-aged) SA substrate in Fig. 2 indicate a root-mean-square (rms) surface roughness of 210 nm. In accordance with previous studies, this rms value will have no significant effect on the contact angle measurements because it is lower than1 μm (Marmur, 2006; Al-Yaseri et al., 2016; Hosseini et al., 2022c). In addition, the approximate pore throat radius is 2.4 nm, and the Brunauer–Emmett–Teller (BET) surface area is 9.67 m^2/g.

The total organic carbon (TOC) contents of the pure and organic-aged SA basalt samples were obtained as 400 mg/L and 700 mg/L respectively. The high TOC of the organic acid-aged SA basalt confirms the adsorption of the organic acid molecules onto the surface of the basalt. Further, the XRD pattern of the pure SA basalt sample in Fig. 3 indicates the presence of the minerals such as anorthite, augite, and albite, with the bulk mineralogy listed in Table 1. Thus, the principal components of the SA basalt are 33% sodium alumina-silicate ($NaAlSi_3O_8$) and 51% calcium alumina-silicate ($CaAl_2Si_2O_8$).

The FESEM micrographs of the pure and nano-treated SA basalts are compared in Fig. 4, where firmly-adhered mono- and multi-layers of SiO_2 nanoparticle clusters are clearly observed on the latter. This is further confirmed by the EDS spectrum of 0.1 wt% nano-modified SA basalt in Fig. 5, which indicates that the composition of the nano-treated basalt is primarily silicon (56%) and oxygen (30%). These results suggest that the SiO_2 nanoparticles are irreversibly adsorbed on the SA basalt, and that these may be capable of reversing the CO_2-wettability to more water-wet conditions.

3.2. The effects of nanoparticles treatment on the CO_2-wettability of SA basalt under various pressures

The effects of various SiO_2 nanofluid concentrations on the θ_a and θ_r measurements at a constant temperature of 323 K under various pressures are presented in Figs. 6 and 7, respectively. Here, both contact angles are seen to increase as the CO_2 pressure is increased. Generally, the pure SA basalt (black profiles, Figs. 6 and 7) maintains its initial water-wet condition under all pressures, while the organic acid-aged SA basalt without the nano-fluid (red profiles, Figs. 6 and 7) is weakly water wet at 0.1 MPa ($\theta_a = 70°$ and $\theta_r = 58°$) and CO_2 wet at higher pressures, with θ_a values of 99.3° and 106.8° at 10 MPa and 20 MPa, respectively. Similarly, at 10 and 20 MPa, the θ_r values of the organic-aged SA basalt are 85.2° and 95.2°, respectively. The increases in θ_a and θ_r with

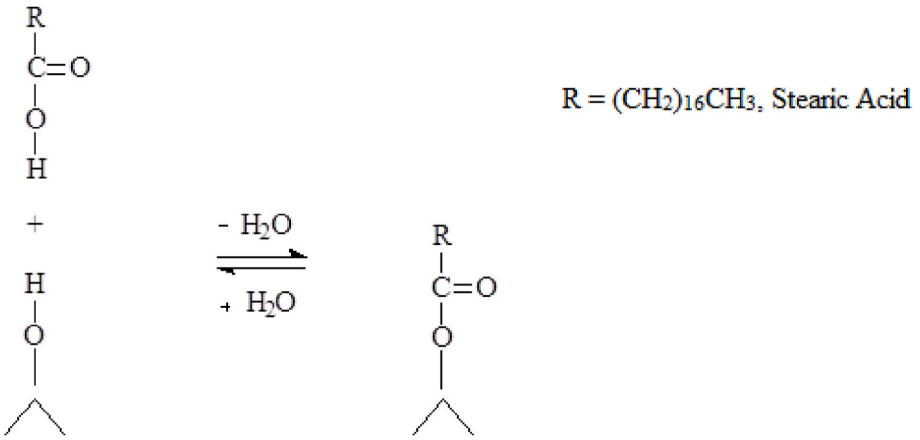

Fig. 1. Chemisorption of organic acid on the solid Saudi Arabian (SA) basalt substrate (∧ represents the solid basalt) (Ali et al., 2019a, 2019b).

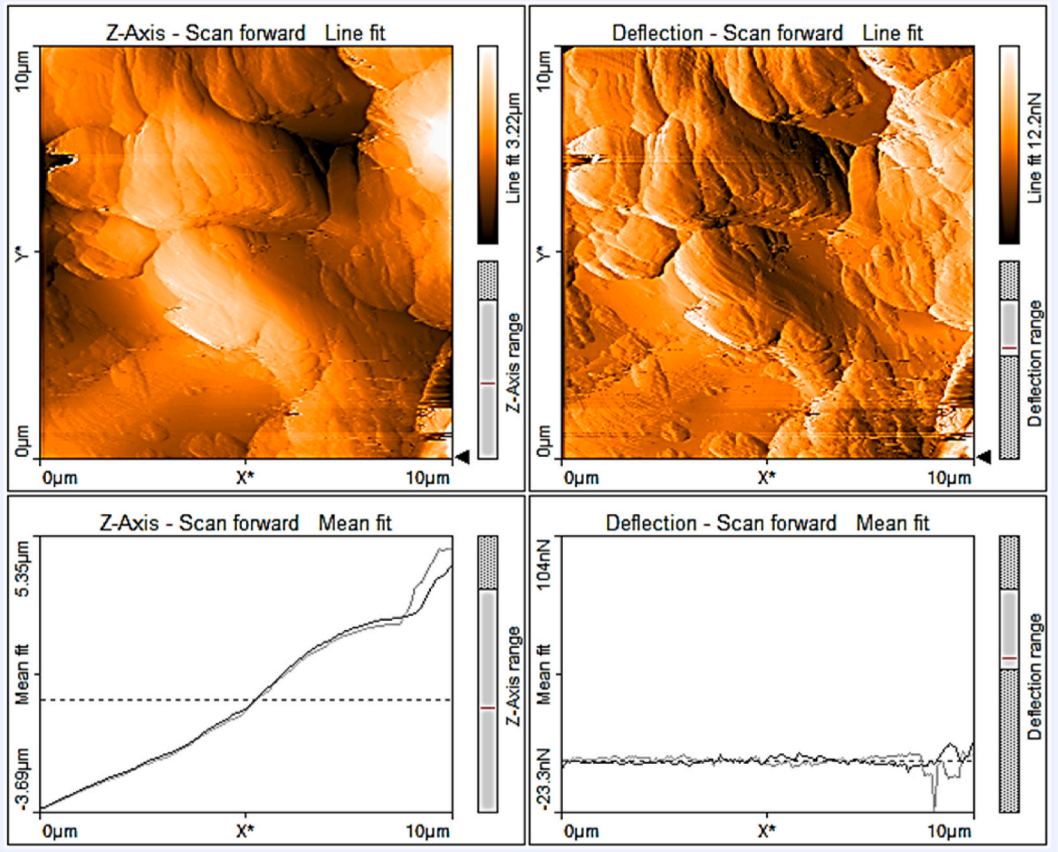

Fig. 2. The AFM images (top) and surface roughness profiles (bottom) of the pure SA basalt.

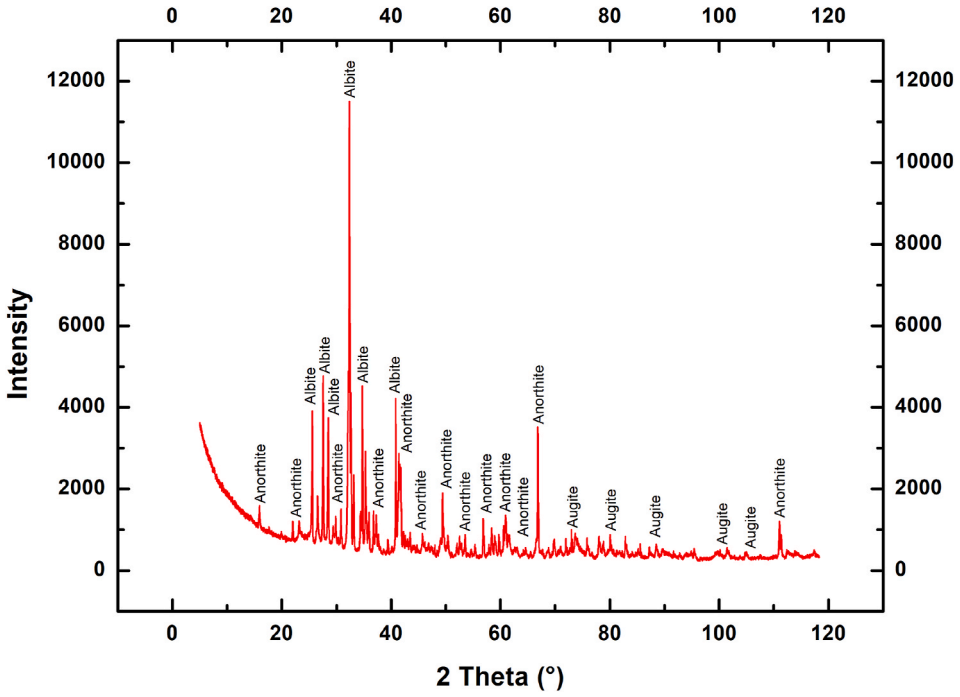

Fig. 3. The XRD pattern of the pure SA basalt.

increased pressure can be attributed to an enhancement in the basalt/CO_2 inter-molecular interactions due to the increase in the density of CO_2 with the increase in pressure. Similar results have been reported for basalt (Iglauer et al., 2020; Al-Yaseri et al., 2021b; Raza et al., 2022) and for other rock and mineral substrates such as calcite and carbonates, mica and shale, quartz and sandstone (Farokhpoor et al., 2013a, 2013b; Kaveh et al., 2014; Arif et al., 2017; Garing and Benson, 2019; Fauziah et al., 2020; Ali et al., 2021b; Baban et al., 2021; Yekeen et al., 2021;

Table 1
The XRD analysis of the pure SA basalt.

Mineral phase	Composition (wt.%)
Anorthite ($CaAl_2Si_2O_8$)	51
Augite [(Ca, Na) (Mg, Fe, Al, Ti) (Si, Al)$_2O_6$]	16
Albite ($NaAlSi_3O_8$)	33

Ivanova et al., 2022).

Hydrophilic (water-wet) rocks are generally more suitable for the residual/structural trapping of CO_2 because an upwardly-directed suction force is initiated through the caprock at contact angles greater than 90°, thus resulting in the leakage of gaseous CO_2 and failure of CO_2 sequestration projects. Moreover, under such conditions, the buoyant force will be higher than the capillary force provided by the capillary pressure (P_c) according to Eq. (1):

$$P_c = P_{CO_2} - P_{water} = \frac{2\gamma \cos(\theta)}{r} \quad (1)$$

where γ is CO_2/brine interfacial tension in mN/m, θ is contact angle in degrees, and r is a capillary radius (pore throat) in meters (m). Thus, the increase in buoyancy pressure over and above the capillary force of the CO_2 plume with increasing rock hydrophobicity will increase the possibility of CO_2 leakages across the caprock at higher pressures. After treatment with various concentrations of SiO_2 nanofluid, however, the SA basalt exhibits strongly water-wet behavior (green profiles, Figs. 6 and 7). Here, at nanofluid concentrations of 0.05–0.75 wt%, all of the θ_a values remain below 77°, while the θ_r values remain below 71°, as the pressure is varied between 0.1 and 20 MPa at the constant temperature of 323 K. This demonstrates that the nanofluids alter the wettability of the organic acid-aged SA basalts to obtain a more hydrophilic condition. This effect is more noticeable in the presence of 0.1 wt% SiO_2 (1000

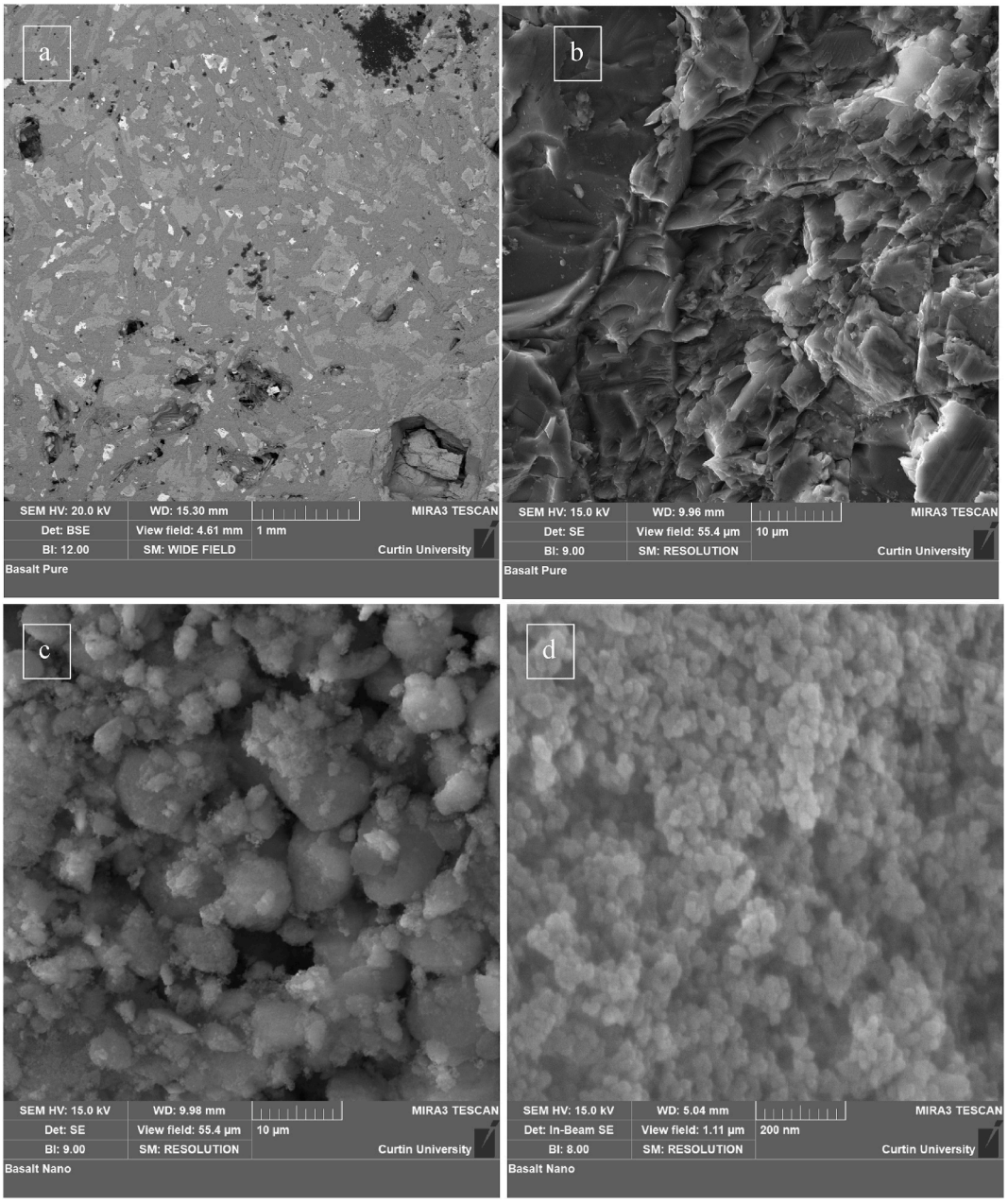

Fig. 4. The FESEM micrographs of (a and b) the pure SA basalt (scale bar = 1 mm and 10 µm, respectively) and (c and d) the SiO_2 nano-treated SA basalt (scale bar = 10 µm and 200 nm, respectively).

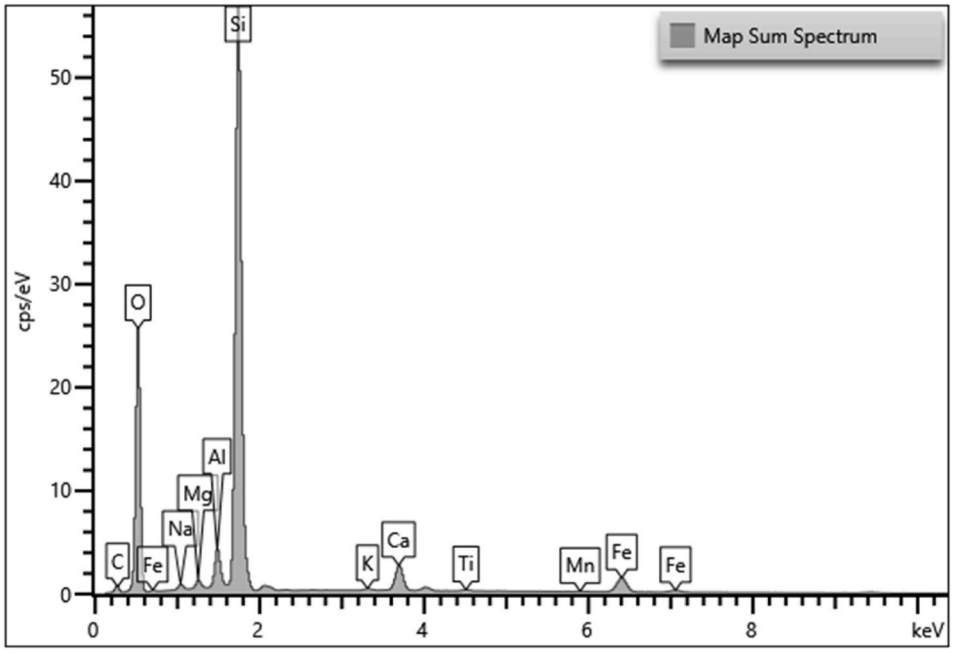

Fig. 5. The EDS spectrum of the 0.1 wt% SiO_2 nano-treated SA basalt.

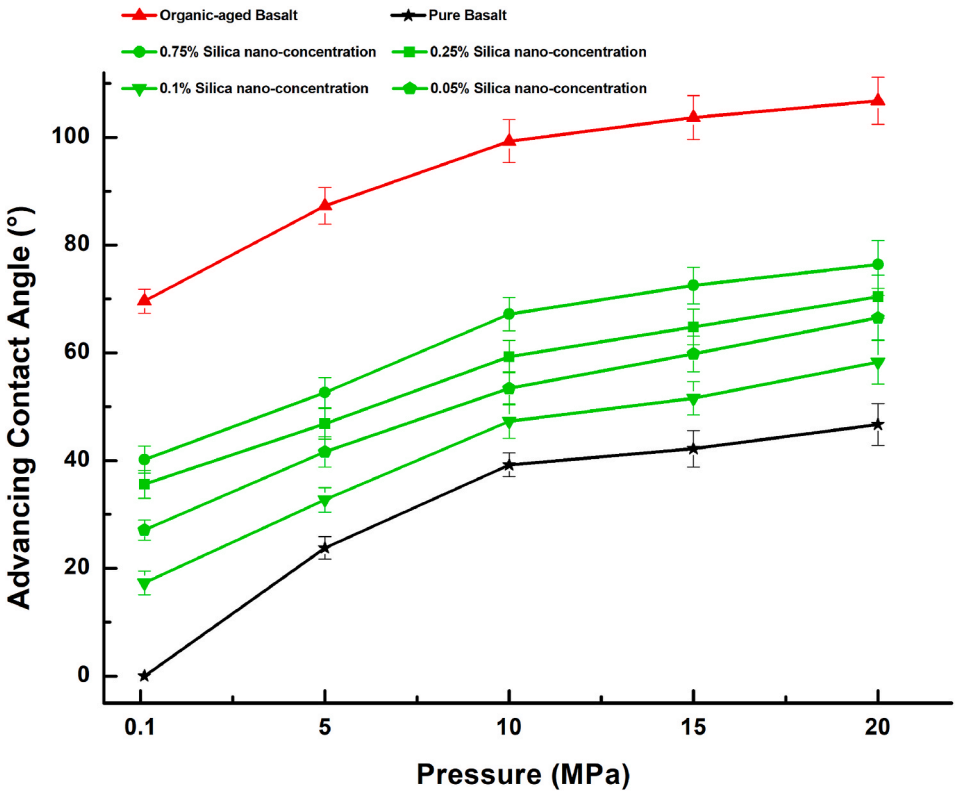

Fig. 6. The advancing contact angle (θ_a) values of the pure SA basalt/CO_2/brine system (black profile), the organic-acid aged SA basalt/CO_2/brine system (red profile), and the various organic-acid/SiO_2 nanofluid aged SA basalt/CO_2/brine systems (green profiles) under various pressures and at a constant temperature of 323 K. (For interpretation of the references to color in this figure legend, the reader is referred to the Web version of this article.)

ppm), where the nanofluid has reversed the CO_2-wettability to more optimal water-wet conditions, giving the greatest reductions in θ_a and θ_r (i.e., the lowest θ_a and θ_r values) relative to those of the organic-aged SA basalt. In other words, the θ_a and θ_r values obtained in the presence of 0.1 wt% SiO_2 are closest to those of the pure (uncontaminated, water wet) SA basalt. By contrast, when the SiO_2 nanofluid concentrations are increased to 0.25 and 0.75 wt%, the advancing and receding contact angles are higher than those obtained with 0.1 wt% under all pressures, although they remain lower than those obtained for the organic-aged basalt in the absence of nanofluid. Notably, the use of 0.05% nanofluid is also less effective than 0.1 wt% for reducing the θ_a and θ_r values. These results suggest that there exists an optimum nanofluid

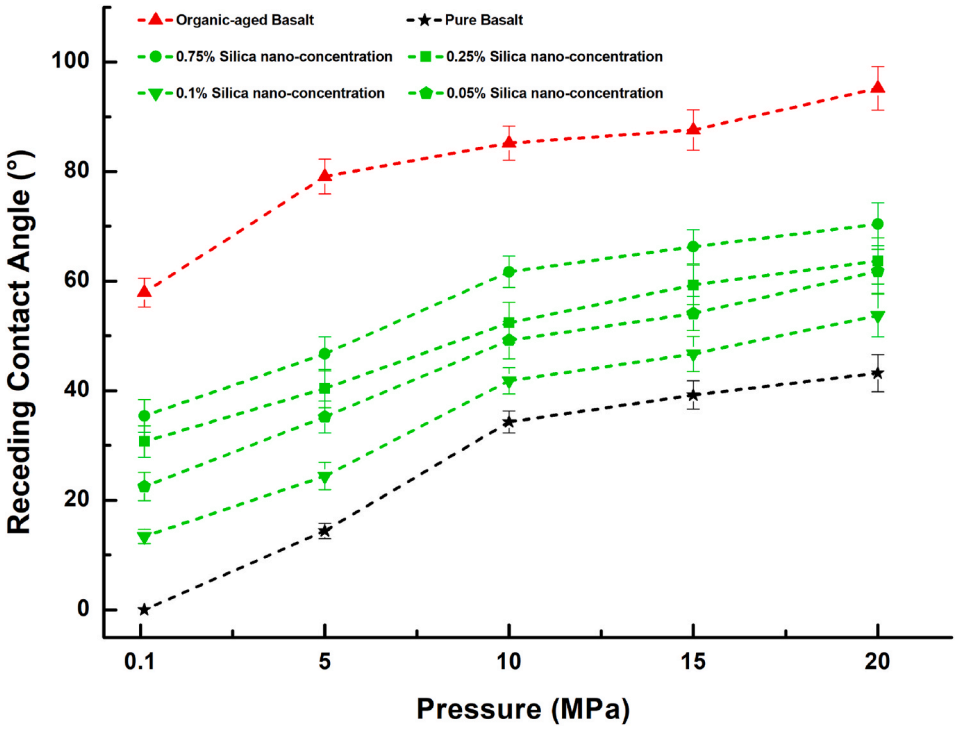

Fig. 7. The receding contact angle (θ_r) values of the pure SA basalt/CO_2/brine system (black profile), the organic-acid aged SA basalt/CO_2/brine system (red profile), and the various organic-acid/SiO_2 nanofluid aged SA basalt/CO_2/brine systems (green profiles) under various pressures and at a constant temperature of 323 K. (For interpretation of the references to color in this figure legend, the reader is referred to the Web version of this article.)

concentration (around 0.1 wt%; due to irreversible adsorption of nanofluid) for mitigating the reduction in the wetting behavior of the SA basalt due to organic-acid aging. The irreversible adsorption of nanofluid is caused by the opposite surface charges of nanofluids and SA basalt. This is further evidenced by the XRD results in Table 1, which reveal the significant presence of divalent cations such as Ca^{2+} and Mg^{2+}, and Fe^{2+}, thus suggesting that the basalt surface is highly positively charged. The electrostatic attraction between the positively charged basalt surface and the negatively charged SiO_2 nanoparticles promotes the adsorption of nanoparticles on the basalt surface. Consequently, the nanofluids irreversibly alter the wettability of the SA basalt towards the hydrophilic state (Ali et al., 2020b, 2021a; Al-Yaseri et al., 2021a; Hosseini et al., 2022a). Thus, it is essential to identify the threshold nanofluid concentration at which the SA basalt can become

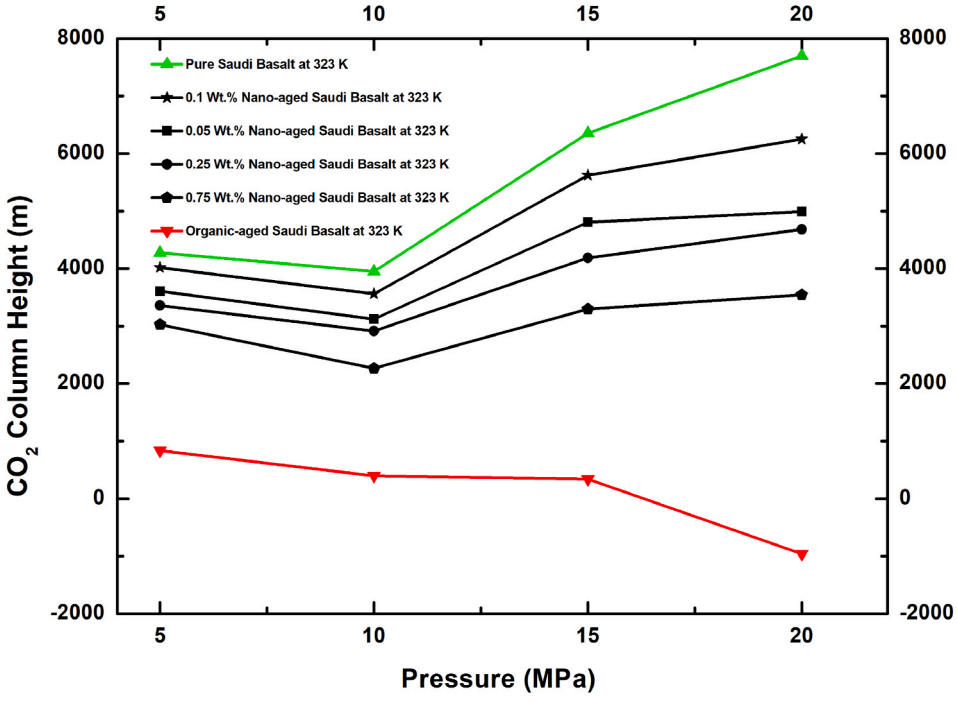

Fig. 8. The CO_2 column heights of the pure, organic-aged, and nanofluid-treated SA basalts at 323 K and various pressures.

strongly water-wet. Such conditions are required in order to improve the residual and structural trapping of CO_2 in SA basaltic formations. This effect is also directly connected to carbon mineralization, where water-wet conditions favor the rapid mineralization rates in SA basalts (Iglauer et al., 2020; Ali et al., 2023).

3.3. The effects of nanoparticles treatment on the CO_2 column heights

For an un-fractured basaltic rock, the capillary entry pressure alone dictates the critical pressure above which a fluid will migrate. In this context, the sealing and mineralization capabilities of the pure, organic acid-aged, and nanofluid-treated SA basalt substrates are evaluated according to the plots of CO_2 column height against pressure in Fig. 8. Here, the pure SA basalt (green profile) exhibits the highest column of CO_2, whereas the structural trapping potential of the rock is considerably reduced in the presence of organic acid (red profile), for which a negative CO_2 column height of −957 m is observed at 20 MPa and 323 K. This corresponds to the negative suction force for the penetration of CO_2 into the geological formation, thereby indicating that CO_2 can percolate in an upward direction from the basaltic formation before any mineralization reaction can occur, thus causing leakage (Iglauer et al., 2015; Espinoza and Santamarina, 2017; Al-Mukainah et al., 2022; Alanazi et al., 2022; Hosseini et al., 2022b). When the SA basalt surface is treated with SiO_2 nanofluid, however, the column height of CO_2 that can be perpetually immobilized under a pressure of 5 MPa is seen to increase significantly from 835 m for the untreated organic-aged basalt (red triangle) to 3027 m with 0.75 wt% (black pentagon), 3361 m with 0.25 wt% (black circle), 3607 m with 0.05 wt% SiO_2 nanofluid (black square), and a maximum of 4020 m after the treatment with 0.1 wt% SiO_2 nanofluid (black star). Thus, the treatment of the organic-aged SA basalt with the SiO_2 nanofluid effectively reverses the rock wettability to almost the same as that of the pure basalt. Moreover, at 20 MPa and 323 K, the optimum nanofluid concentration of 0.1 wt% gives a CO_2 column height of 6253 m, which contrasts significantly with the highly negative value of the untreated basalt due to organic acid contamination.

As well as confirming that the optimum CO_2 column height performance is obtained with 0.1 wt% SiO_2, the results in Fig. 8 also demonstrate that the CO_2 column heights of both the pure and nano-treated basalts increase with increasing pressure, whereas the opposite trend is observed for the stearic acid-aged SA basalt without the nanofluid treatment. These results further demonstrate that the likelihood of CO_2 leakage across the basaltic formation will be decreased, and the CO_2 trapping potential and mineralization rate of the formation will be increased, by the treatment with SiO_2 nanofluids.

4. Conclusions

The CO_2 capture and sequestration in geological formations is an exemplary process for minimizing global warming and achieving a CO_2-free global economy (Al-Anssari et al., 2017; Jha et al., 2018; Arif et al., 2019; Fauziah et al., 2020; Ali et al., 2022a; Aslannezhad et al., 2023). In Saudi Arabian (SA) basalt, industrial-scale CO_2 storage can be achieved via rock surface mineralization (Gislason et al., 2010; Snæbjörnsdóttir et al., 2014; Al-Khdheeawi et al., 2020; Arkadakskiy et al., 2020; Torres, 2020; Abdulelah et al., 2021; Oelkers et al., 2022). However, such mineralization procedures are significantly impacted by changes in the wettability of the basalt surface due to ubiquitous contamination with organic acids (Al-Yaseri et al., 2021a; Ali et al., 2023). Moreover, the residual/capillary and structural trapping of basalt also depends on rock wettability (Rahman et al., 2016; Al-Khdheeawi et al., 2017a, 2017b). Hence, the present study examined the feasibility of altering the surfaces of organic acid-aged SA basalts from hydrophobic to hydrophilic conditions via treatment with various concentrations of SiO_2 nanofluids. Further, the effects of these treatments on the CO_2 mineralization procedures, along with the capillary and structural trapping capacities, were investigated herein. The advancing and retreating contact angles (θ_a and θ_r) of the pure, organic acid-aged, and nanofluid-treated SA basalt substrates were measured under reservoir conditions (i.e., a temperature of 323 K and pressures of 0.1–20 MPa). The results indicated that while the pure SA basalt was strongly water wet, the organic acid-aged SA basalt was hydrophobic and CO_2 wet. After treatment with SiO_2 nanofluids, the SA basalt was significantly altered to weakly water-wet and intermediate-wet conditions, depending on the nanofluid concentration. The optimum SiO_2 nanofluid concentration for attaining a maximum increase in water wettability was found to be 0.1 wt%.

For the organic-aged basalt in the absence of nanofluid, the column height of CO_2 corresponding to the capillary entry pressure was shown to decrease from 835 to a negative value of −957 m as the pressure increased from 5 to 20 MP. After treatment of the SA basalt with SiO_2 nanofluid, however, highly positive column heights were observed, especially at higher pressures, with the 0.1 wt% nano-treatment giving the greatest CO_2 column height of 6253 m at 20 MPa. This result strongly suggests that the risk of CO_2 seepage can be reduced by the nanofluid treatment. Moreover, the CO_2 trapping potentials of SA basaltic formations can be increased by the nanofluid treatment. The scanning electron microscope (SEM) analysis revealed the presence of clusters of agglomerated nanoparticles on the surface of nano-aged SA basalt, thereby suggesting that the nanoparticles are strongly adsorbed due to electrostatic attractions between the positive charges on the basalt surface and the negative charges on the SiO_2 nanoparticles, which permanently altered the wetting characteristics. In brief, the modification of organic acid-aged SA basalt by treatment with SiO_2 nanofluid can significantly and positively influence CO_2 mineralization procedures, along with the capillary and structural trapping of CO_2 in SA basaltic formations.

Credit author statement

Muhammad Ali: Conceptualization, Methodology, Validation, Investigation, Data Curation, Writing - Original Draft, Writing - Review & Editing; Nurudeen Yekeen: Visualization, Writing - Review & Editing; Mirhasan Hosseini: Validation, Formal analysis; Ghazanfer Raza Abbasi: Software, Validation; Amer Alanazi: Visualization, Writing - Review & Editing; Alireza Keshavarz: Data Curation, Methodology; Thomas Finkbeiner: Validation, Writing - Review & Editing; Hussein Hoteit: Resources, Writing - Review & Editing, Project administration, Supervision.

Declaration of competing interest

The authors declare that they have no known competing financial interests or personal relationships that could have appeared to influence the work reported in this paper.

Data availability

All the related data is already presented in the article

Acknowledgment

This publication is supported by the King Abdullah University of Science and Technology (KAUST) Research Funding Office under Award No. 4357.

References

Abbasi, G.R., Arif, M., Isah, A., Ali, M., Mahmoud, M., Hoteit, H., Keshavarz, A., Iglauer, S., 2022. Gas hydrate characterization in sediments via x-ray microcomputed tomography. Earth Sci. Rev., 104233

Abdulelah, H., Al-Yaseri, A., Ali, M., Giwelli, A., Negash, B.M., Sarmadivaleh, M., 2021. CO2/Basalt's interfacial tension and wettability directly from gas density: implications for Carbon Geo-sequestration. J. Petrol. Sci. Eng. 204, 108683.

Agboola, M.O., Bekun, F.V., Joshua, U., 2021. Pathway to environmental sustainability: nexus between economic growth, energy consumption, CO2 emission, oil rent and total natural resources rent in Saudi Arabia. Resour. Pol. 74, 102380.
Akob, D.M., Cozzarelli, I.M., Dunlap, D.S., Rowan, E.L., Lorah, M.M., 2015. Organic and inorganic composition and microbiology of produced waters from Pennsylvania shale gas wells. Appl. Geochem. 60, 116–125.
Al-Anssari, S., Nwidee, L., Ali, M., Sangwai, J.S., Wang, S., Barifcani, A., Iglauer, S., 2017. Retention of Silica Nanoparticles in Limestone Porous Media. SPE/IATMI Asia Pacific Oil & Gas Conference and Exhibition. Society of Petroleum Engineers.
Al-Anssari, S., Arif, M., Wang, S., Barifcani, A., Lebedev, M., Iglauer, S., 2018. Wettability of nanofluid-modified oil-wet calcite at reservoir conditions. Fuel 211, 405–414.
Al-Anssari, S., Arain, Z.U.A., Shanshool, H.A., Ali, M., Keshavarz, A., Iglauer, S., Sarmadivaleh, M., 2020, November. Effect of nanoparticles on the interfacial tension of CO2-oil system at high pressure and temperature: An experimental approach. In: SPE Asia Pacific Oil & Gas Conference and Exhibition. OnePetro.
Al-Khdheeawi, E.A., Vialle, S., Barifcani, A., Sarmadivaleh, M., Iglauer, S., 2017a. Impact of reservoir wettability and heterogeneity on CO2-plume migration and trapping capacity. Int. J. Greenh. Gas Control 58, 142–158.
Al-Khdheeawi, E.A., Vialle, S., Barifcani, A., Sarmadivaleh, M., Iglauer, S., 2017b. Influence of injection well configuration and rock wettability on CO2 plume behaviour and CO2 trapping capacity in heterogeneous reservoirs. J. Nat. Gas Sci. Eng. 43, 190–206.
Al-Khdheeawi, E.A., Mahdi, D.S., Ali, M., Fauziah, C.A., Barifcani, A., 2020. Impact of caprock type on geochemical reactivity and mineral trapping efficiency of CO2. In: Offshore Technology Conference Asia. OnePetro.
Al-Khdheeawi, E.A., Mahdi, D.S., Ali, M., Iglauer, S., Barifcani, A., 2021. Reservoir Scale Porosity-Permeability Evolution in Sandstone Due to CO2 Geological Storage. Available at SSRN 3818887.
Al-Mukainah, H., Al-Yaseri, A., Yekeen, N., Al Hamad, J., Mahmoud, M., 2022. Wettability of shale–brine–H2 system and H2-brine interfacial tension for assessment of the sealing capacities of shale formations during underground hydrogen storage. Energy Rep. 8, 8830–8843.
Al-Yaseri, A.Z., Lebedev, M., Barifcani, A., Iglauer, S., 2016. Receding and advancing (CO2+ brine+ quartz) contact angles as a function of pressure, temperature, surface roughness, salt type and salinity. J. Chem. Therm. 93, 416–423.
Al-Yaseri, A., Abdulelah, H., Yekeen, N., Ali, M., Negash, B.M., Zhang, Y., 2021. Assessment of CO2/shale interfacial tension. Colloids and Surfaces A: Physicochemical and Engineering Aspects 627, 127118.
Al-Yaseri, A., Ali, M., Abbasi, G.R., Abid, H.R., Jha, N.K., 2021a. Enhancing CO2 storage capacity and containment security of basaltic formation using silica nanofluids. Int. J. Greenh. Gas Control 112, 103516.
Al-Yaseri, A., Ali, M., Ali, M., Taheri, R., Wolff-Boenisch, D., 2021b. Western Australia basalt-CO2-brine wettability at geo-storage conditions. J. Colloid Interface Sci. 603, 165–171.
Al-Yaseri, A., Yekeen, N., Ali, M., Pal, N., Verma, A., Abdulelah, H., Hoteit, H., Sarmadivaleh, M., 2022. Effect of organic acids on CO2-rock and water-rock interfacial tension: implications for CO2 geo-storage. J. Petrol. Sci. Eng. 214, 110480.
Alanazi, A., Ali, M., Mowafi, M., Hoteit, H., 2022. Effect of Organics and Nanofluids on Capillary-Sealing Efficiency of Caprock for Hydrogen and Carbon-Dioxide Geological Storage. ARMA/DGS/SEG International Geomechanics Symposium, OnePetro.
Alanazi, A., Abid, H.R., Usman, M., Ali, M., Keshavarz, A., Vahrenkamp, V., Iglauer, S., Hoteit, H., 2023. Hydrogen, carbon dioxide, and methane adsorption potential on Jordanian organic-rich source rocks: implications for underground H2 storage and retrieval. Fuel 346, 128362.
Alhamad, F., Ali, M., Ali, M., Abid, H., Hoteit, H., Iglauer, S., Keshavarz, A., 2022. Effect of methyl orange on wettability of sandstone formations: implications for enhanced oil recovery. Energy Rep. 8, 12357–12365.
Alhamad, F., Sedev, R., Ali, M., Ali, M., Hoteit, H., Iglauer, S., Keshavarz, A., 2023. Effect of Methyl Orange on the Hydrogen Wettability of Sandstone Formation for Enhancing the Potential of Underground Hydrogen Storage. Energy & Fuels.
Ali, M., 2018. Effect of Organic Surface Concentration on CO2-Wettability of Reservoir Rock. Curtin University.
Ali, M., 2021. Effect of Organics and Nanoparticles on CO2-Wettability of Reservoir Rock; Implications for CO2 Geo-Storage. Curtin University.
Ali, M., Al-Anssari, S., Shakeel, M., Arif, M., Dahraj, N.U., Iglauer, S., 2017. Influence of miscible CO 2 flooding on wettability and asphaltene precipitation in Indiana lime stone. In: SPE/IATMI Asia Pacific Oil & Gas Conference and Exhibition. Society of Petroleum Engineers.
Ali, M., Al-Anssari, S., Arif, M., Barifcani, A., Sarmadivaleh, M., Stalker, L., Lebedev, M., Iglauer, S., 2019a. Organic acid concentration thresholds for ageing of carbonate minerals: implications for CO2 trapping/storage. J. Colloid Interface Sci. 534, 88–94.
Ali, M., Al-Anssari, S., Shakeel, M., Arif, M., Dahraj, N.U., Iglauer, S., 2017 October. Influence of miscible CO2 flooding on wettability and asphaltene precipitation in Indiana lime stone. In: *SPE/IATMI Asia Pacific Oil & Gas Conference and Exhibition*. OnePetro.
Ali, M., Arif, M., Sahito, M.F., Al-Anssari, S., Keshavarz, A., Barifcani, A., Stalker, L., Sarmadivaleh, M., Iglauer, S., 2019b. CO2-wettability of sandstones exposed to traces of organic acids: implications for CO2 geo-storage. Int. J. Greenh. Gas Control 83, 61–68.
Ali, M., Aftab, A., Arain, Z.-U.-A., Al-Yaseri, A., Roshan, H., Saeedi, A., Iglauer, S., Sarmadivaleh, M., 2020a. Influence of organic acid concentration on wettability alteration of cap-rock: implications for CO2 trapping/storage. ACS Appl. Mater. Interfaces 12, 39850–39858.
Ali, M., Sahito, M.F., Jha, N.K., Memon, S., Keshavarz, A., Iglauer, S., Saeedi, A., Sarmadivaleh, M., 2020b. Effect of nanofluid on CO2-wettability reversal of sandstone formation; implications for CO2 geo-storage. J. Colloid Interface Sci. 559, 304–312.
Ali, M., Aftab, A., Awan, F.U.R., Akhondzadeh, H., Keshavarz, A., Saeedi, A., Iglauer, S., Sarmadivaleh, M., 2021a. CO2-wettability reversal of cap-rock by alumina nanofluid: implications for CO2 geo-storage. Fuel Process. Technol. 214, 106722.
Ali, M., Awan, F.U.R., Ali, M., Al-Yaseri, A., Arif, M., Sánchez-Román, M., Keshavarz, A., Iglauer, S., 2021b. Effect of humic acid on CO2-wettability in sandstone formation. J. Colloid Interface Sci. 588, 315–325.
Ali, M., Jha, N.K., Al-Yaseri, A., Zhang, Y., Iglauer, S., Sarmadivaleh, M., 2021c. Hydrogen wettability of quartz substrates exposed to organic acids; Implications for hydrogen trapping/storage in sandstone reservoirs. J. Petrol. Sci. Eng., 109081
Ali, M., Yekeen, N., Pal, N., Keshavarz, A., Iglauer, S., Hoteit, H., 2021d. Influence of pressure, temperature and organic surface concentration on hydrogen wettability of caprock; implications for hydrogen geo-storage. Energy Rep. 7, 5988–5996.
Ali, M., Jha, N.K., Pal, N., Keshavarz, A., Hoteit, H., Sarmadivaleh, M., 2022a. Recent advances in carbon dioxide geological storage, experimental procedures, influencing parameters, and future outlook. Earth Sci. Rev. 225, 103895.
Ali, M., Pan, B., Yekeen, N., Al-Anssari, S., Al-Anazi, A., Keshavarz, A., Hoteit, H., 2022b. Assessment of wettability and rock-fluid interfacial tension of caprock: Implications for hydrogen and carbon dioxide geo-storage. International Journal of Hydrogen Energy 47 (30), 14104–14120.
Ali, M., Yekeen, N., Ali, M., Hosseini, M., Pal, N., Keshavarz, A., Iglauer, S., Hoteit, H., 2022c. Effects of Various Solvents on Adsorption of Organics for Porous and Nonporous Quartz/CO2: Implications for CO2 Geo-Storage. Energy & Fuels.
Ali, M., Yekeen, N., Pal, N., Keshavarz, A., Iglauer, S., Hoteit, H., 2022d. Influence of organic molecules on wetting characteristics of mica/H2/brine systems: implications for hydrogen structural trapping capacities. J. Colloid Interface Sci. 608, 1739–1749.
Ali, M., Yekeen, N., Alanazi, A., Keshavarz, A., Iglauer, S., Finkbeiner, T., Hoteit, H., 2023. Saudi Arabian basalt/CO2/brine wettability: implications for CO2 geo-storage. J. Energy Storage 62, 106921.
Arif, M., Lebedev, M., Barifcani, A., Iglauer, S., 2017. CO2 storage in carbonates: wettability of calcite. Int. J. Greenh. Gas Control 62, 113–121.
Arif, M., Abu-Khamsin, S., Iglauer, S., 2019. Wettability of rock/CO2/brine and rock/oil/CO2-enriched-brine systems: critical parametric analysis and future outlook. Adv. Colloid Interface Sci. 268, 91–113.
Arkadakskiy, S., Oelkers, E., Afifi, A., Hoteit, H., Gíslason, S., Kunnummal, N., Ahmed, Z., 2020. The Potential for Sequestering CO 2 in Basalts along the Red Sea Coast of Saudi Arabia. AGU Fall Meeting Abstracts. GC111-105.
Aslannezhad, M., Ali, M., Kalantariasl, A., Sayyafzadeh, M., You, Z., Iglauer, S., Keshavarz, A., 2023. A review of hydrogen/rock/brine interaction: implications for Hydrogen Geo-storage. Prog. Energy Combust. Sci. 95, 101066.
Awan, F.U.R., Keshavarz, A., Azhar, M.R., Akhondzadeh, H., Ali, M., Al-Yaseri, A., Abid, H.R., Iglauer, S., 2021. Adsorption of nanoparticles on glass bead surface for enhancing proppant performance: a systematic experimental study. J. Mol. Liq. 328, 115398.
Baban, A., Al-Yaseri, A., Keshavarz, A., Amin, R., Iglauer, S., 2021. CO2–brine–sandstone wettability evaluation at reservoir conditions via Nuclear Magnetic Resonance measurements. Int. J. Greenh. Gas Control 111, 103435.
Bamisile, O., Wang, X., Adun, H., Ejiyi, C.J., Obiora, S., Huang, Q., Hu, W., 2022. A 2030 and 2050 feasible/sustainable decarbonization perusal for China's Sichuan Province: a deep carbon neutrality analysis and EnergyPLAN. Energy Convers. Manag. 261, 115605.
Bikkina, P.K., 2011. Contact angle measurements of CO2–water–quartz/calcite systems in the perspective of carbon sequestration. Int. J. Greenh. Gas Control 5, 1259–1271.
Blunt, M., Jr, F.J.F., Orr, F.M., 1993. Carbon dioxide in enhanced oil recovery. Energy Convers. Manag. 34, 9–11.
Cao, C., Liu, H., Hou, Z., Mehmood, F., Liao, J., Feng, W., 2020. A review of CO2 storage in view of safety and cost-effectiveness. Energies 13, 600.
Coleman, R.G., Gregory, R., Brown, G.F., 1983. Cenozoic Volcanic Rocks of Saudi Arabia. US Department of the Interior, Geological Survey.
Daryasafar, A., Keykhosravi, A., Shahbazi, K., 2019. Modeling CO2 wettability behavior at the interface of brine/CO2/mineral: application to CO2 geo-sequestration. J. Clean. Prod. 239, 118101.
Delshad, M., Umurzakov, Y., Sepehrnoori, K., Eichhubl, P., Batista Fernandes, B.R., 2022. Hydrogen storage assessment in depleted oil reservoir and saline aquifer. Energies 15, 8132.
El-Maghraby, R., Pentland, C., Iglauer, S., Blunt, M., 2012. A fast method to equilibrate carbon dioxide with brine at high pressure and elevated temperature including solubility measurements. J. Supercrit. Fluids 62, 55–59.
Espinoza, D.N., Santamarina, J.C., 2017. CO2 breakthrough—caprock sealing efficiency and integrity for carbon geological storage. Int. J. Greenh. Gas Control 66, 218–229.
Farokhpoor, R., Bjørkvik, B.J., Lindeberg, E., Torsæter, O., 2013a. CO2 wettability behavior during CO2 sequestration in saline aquifer-An Experimental study on minerals representing sandstone and carbonate. Energy Proc. 37, 5339–5351.
Farokhpoor, R., Bjørkvik, B.J., Lindeberg, E., Torsæter, O., 2013b. Wettability behaviour of CO2 at storage conditions. Int. J. Greenh. Gas Control 12, 18–25.
Fauziah, C.A., Al-Yaseri, A.Z., Jha, N.K., Lagat, C., Roshan, H., Barifcani, A., Iglauer, S., 2020. Carbon dioxide wettability of south west hub sandstone, western Australia: implications for carbon geo-storage. Int. J. Greenh. Gas Control 98, 103064.
Garing, C., Benson, S., 2019. CO2 wettability of sandstones: addressing conflicting capillary behaviors. Geophys. Res. Lett. 46, 776–782.
Gislason, S.R., Wolff-Boenisch, D., Stefansson, A., Oelkers, E.H., Gunnlaugsson, E., Sigurdardottir, H., Sigfusson, B., Broecker, W.S., Matter, J.M., Stute, M., 2010. Mineral sequestration of carbon dioxide in basalt: a pre-injection overview of the CarbFix project. Int. J. Greenh. Gas Control 4, 537–545.

Hamieh, A., Rowaihy, F., Al-Juaied, M., Abo-Khatwa, A.N., Afifi, A.M., Hoteit, H., 2022. Quantification and analysis of CO2 footprint from industrial facilities in Saudi Arabia. Energy Convers. Manag. X 16, 100299.
Hosseini, M., Ali, M., Fahimpour, J., Keshavarz, A., Iglauer, S., 2022a. Basalt-H2-brine wettability at geo-storage conditions: implication for hydrogen storage in basaltic formations. J. Energy Storage 52, 104745.
Hosseini, M., Fahimpour, J., Ali, M., Keshavarz, A., Iglauer, S., 2022b. Capillary Sealing Efficiency Analysis of Caprocks: Implication for Hydrogen Geological Storage. Energy & Fuels.
Hosseini, M., Fahimpour, J., Ali, M., Keshavarz, A., Iglauer, S., 2022c. Hydrogen wettability of carbonate formations: Implications for hydrogen geo-storage. Journal of Colloid and Interface Science 614, 256–266.
Hosseini, M., Ali, M., Fahimpour, J., Keshavarz, A., Iglauer, S., 2023. Calcite–Fluid Interfacial Tension: H2 and CO2 Geological Storage in Carbonates. Energy & Fuels.
Iglauer, S., 2017. CO2–water–rock wettability: variability, influencing factors, and implications for CO2 geostorage. Acc. Chem. Res. 50, 1134–1142.
Iglauer, S., Pentland, C., Busch, A., 2015. CO2 wettability of seal and reservoir rocks and the implications for carbon geo-sequestration. Water Resour. Res. 51, 729–774.
Iglauer, S., Al-Yaseri, A.Z., Wolff-Boenisch, D., 2020. Basalt-CO2-brine wettability at storage conditions in basaltic formations. Int. J. Greenh. Gas Control 102, 103148.
Iglauer, S., Ali, M., Keshavarz, A., 2021. Hydrogen wettability of sandstone reservoirs: implications for hydrogen geo-storage. Geophys. Res. Lett. 48, e2020GL090814.
Ivanova, A., Orekhov, A., Markovic, S., Iglauer, S., Grishin, P., Cheremisin, A., 2022. Live imaging of micro and macro wettability variations of carbonate oil reservoirs for enhanced oil recovery and CO2 trapping/storage. Sci. Rep. 12, 1–12.
Jha, N., Ali, M., Sarmadivaleh, M., Iglauer, S., Barifcani, A., Lebedev, M., Sangwai, J., 2018. Low salinity surfactant nanofluids for enhanced CO2 storage application at high pressure and temperature. In: Fifth CO2 Geological Storage Workshop. European Association of Geoscientists & Engineers, pp. 1–4.
Jones, D., Head, I., Gray, N., Adams, J., Rowan, A., Aitken, C., Bennett, B., Huang, H., Brown, A., Bowler, B., 2008. Crude-oil biodegradation via methanogenesis in subsurface petroleum reservoirs. Nature 451, 176–180.
Kang, M., Kim, J.H., Kim, K.-O., Cheong, S., Shinn, Y.J., 2018. Assessment of CO2 Storage Capacity for Basalt Caprock-Sandstone Reservoir System in the Northern East China Sea. EGU General Assembly Conference Abstracts, p. 5772.
Kaveh, N.S., Rudolph, E., Van Hemert, P., Rossen, W., Wolf, K.-H., 2014. Wettability evaluation of a CO2/water/bentheimer sandstone system: contact angle, dissolution, and bubble size. Energy Fuel. 28, 4002–4020.
Kelemen, P., Benson, S.M., Pilorgé, H., Psarras, P., Wilcox, J., 2019. An overview of the status and challenges of CO2 storage in minerals and geological formations. Frontiers in Climate 1, 9.
Khalifa, A.A., Ibrahim, A.-J., Amhamed, A.I., El-Naas, M.H., 2022. Accelerating the transition to a circular economy for net-zero emissions by 2050: a systematic review. Sustainability 14, 11656.
Lander, L.M., Siewierski, L.M., Brittain, W.J., Vogler, E.A., 1993. A systematic comparison of contact angle methods. Langmuir 9, 2237–2239.
Le, T.T.B., Striolo, A., Cole, D.R., 2020. Supercritical CO2 effects on calcite wettability: a molecular perspective. J. Phys. Chem. C 124, 18532–18543.
Lundegard, P.D., Kharaka, Y.K., 1994. Distribution and occurrence of organic acids in subsurface waters. In: Organic Acids in Geological Processes. Springer, pp. 40–69.
Mahesar, A.A., Ali, M., Shar, A.M., Memon, K.R., Mohanty, U.S., Akhondzadeh, H., Tunio, A.H., Iglauer, S., Keshavarz, A., 2020. Effect of cryogenic liquid nitrogen on the morphological and petrophysical characteristics of tight gas sandstone rocks from kirthar fold belt, Indus Basin, Pakistan. Energy Fuel. 34, 14548–14559.
Marmur, A., 2006. Soft contact: measurement and interpretation of contact angles. Soft Matter 2, 12–17.
Matter, J.M., Stute, M., Snæbjörnsdottir, S.Ó., Oelkers, E.H., Gislason, S.R., Aradottir, E. S., Sigfusson, B., Gunnarsson, I., Sigurdardottir, H., Gunnlaugsson, E., 2016. Rapid carbon mineralization for permanent disposal of anthropogenic carbon dioxide emissions. Science 352, 1312–1314.
Moufti, M.R., Németh, K., 2016. Harrat Rahat: the geoheritage value of the youngest long-lived volcanic field in the Kingdom of Saudi Arabia. In: Geoheritage of Volcanic Harrats in Saudi Arabia. Springer, pp. 33–120.
Nwidee, L., Al-Anssari, S., Barifcani, A., Sarmadivaleh, M., Iglauer, S., 2016. Nanofluids for Enhanced Oil Recovery Processes: Wettability Alteration Using Zirconium Oxide. Offshore Technology Conference Asia, OnePetro.
Oelkers, E.H., Arkadakskiy, S., Afifi, A.M., Hoteit, H., Richards, M., Fedorik, J., Delaunay, A., Torres, J.E., Ahmed, Z.T., Kunnummal, N., 2022. The subsurface carbonation potential of basaltic rocks from the Jizan region of Southwest Saudi Arabia. Int. J. Greenh. Gas Control 120, 103772.
Raad, S.M.J., Leonenko, Y., Hassanzadeh, H., 2022. Hydrogen storage in saline aquifers: opportunities and challenges. Renew. Sustain. Energy Rev. 168, 112846.
Rahman, T., Lebedev, M., Barifcani, A., Iglauer, S., 2016. Residual trapping of supercritical CO2 in oil-wet sandstone. J. Colloid Interface Sci. 469, 63–68.
Raza, A., Glatz, G., Gholami, R., Mahmoud, M., Alafnan, S., 2022. Carbon mineralization and geological storage of CO2 in basalt: mechanisms and technical challenges. Earth Sci. Rev. 229, 104036.
Silvestri, A., Ataman, E., Budi, A., Stipp, S., Gale, J.D., Raiteri, P., 2019. Wetting properties of the CO2–water–calcite system via molecular simulations: shape and size effects. Langmuir 35, 16669–16678.
Snæbjörnsdóttir, S.Ó., Wiese, F., Fridriksson, T., Ármansson, H., Einarsson, G.M., Gislason, S.R., 2014. CO2 storage potential of basaltic rocks in Iceland and the oceanic ridges. Energy Proc. 63, 4585–4600.
Torres, J.E.A., 2020. The Potential for CO2 Disposal in Western Saudi Arabia: the Jizan Group Basalts.
Wang, S., Zhou, G., Ma, Y., Gao, L., Song, R., Jiang, G., Lu, G., 2016. Molecular dynamics investigation on the adsorption behaviors of H2O, CO2, CH4 and N2 gases on calcite (1 1 0) surface. Appl. Surf. Sci. 385, 616–621.
Wang, T., Jiang, Z., Zhao, B., Gu, Y., Liou, K.-N., Kalandiyur, N., Zhang, D., Zhu, Y., 2020. Health co-benefits of achieving sustainable net-zero greenhouse gas emissions in California. Nat. Sustain. 3, 597–605.
Yekeen, N., Padmanabhan, E., Thenesh, A., Sevoo, L., Kamalarasan, A., Kanesen, L., Okunade, O.A., 2020. Wettability of rock/CO2/brine systems: a critical review of influencing parameters and recent advances. J. Ind. Eng. Chem. 88, 1–28.
Yekeen, N., Padmanabhan, E., Abdulelah, H., Irfan, S.A., Okunade, O.A., Khan, J.A., Negash, B.M., 2021. CO2/brine interfacial tension and rock wettability at reservoir conditions: a critical review of previous studies and case study of black shale from Malaysian formation. J. Petrol. Sci. Eng. 196, 107673.